

## A REVIEW ON MACHINE VISION AND IMAGE PROCESSING TECHNIQUES FOR WEED DETECTION IN AGRICULTURAL CROPS

Rameen Sohail<sup>1</sup>, Qamar Nawaz<sup>2,\*</sup>, Isma Hamid<sup>3,\*</sup>, Syed Mushhad Mustuzhar Gilani<sup>4</sup>, Imran Mumtaz<sup>5</sup>, Ahmad Mateen<sup>6</sup> and Junaid Nawaz<sup>7</sup>

<sup>1,2,5,6</sup>Department of Computer Science, University of Agriculture, Faisalabad, Punjab, Pakistan. <sup>3</sup>Department of Computer Science, National Textile University Faisalabad, Punjab, Pakistan. <sup>4</sup>University Institute of Information Technology, PMAS-Arid Agriculture University Rawalpindi, Punjab, Pakistan. <sup>5</sup>Water Management Research Center, University of Agriculture, Faisalabad, Punjab, Pakistan

\*Corresponding author's e-mail: qamar@uaf.edu.pk; ismahamid@ntu.edu.pk

The advancement in the field of precision agriculture has opened doors for site-specific weed management. There is a growing need to control the amount of herbicide sprayed on weeds to reduce economic and environmental losses. In the field of precision agriculture, incorporation of machine learning techniques has enabled the farmers to automate the process of controlling weed using an adequate number of herbicides for different species in-situ. This study aims to explore various parameters of Computer Vision and Machine Learning algorithms and methods used by researchers to develop Artificial Intelligence models to remove weeds from agricultural fields. More than twenty state-of-the-art algorithms have been studied in this paper. We categorized these algorithms into five categories based on different features i.e. visual, shape, spatial, and spectral. At the end of this study, a comprehensive table is presented containing details of algorithms in terms of limitations and accuracy.

**Keywords:** Image Processing, Weed Detection, Machine Vision, Robotic Weed Control.

### INTRODUCTION

The global population is increasing at an astounding rate that gives rise to the growing need for food, fuel, and fiber. This, in turn, escalated the agricultural requirements for providing higher yields of food and fiber crops. In the same way, more fuel and electricity are required to run heavy agricultural machinery and to produce chemicals and fertilizers. By 2050, the expected number for the global population will be about 9.8 billion (Jones, 2017). Hence, the production level must be doubled accordingly to meet the inflating demands of food and other resources (Cheng and Matson, 2015; Singh *et al.*, 2016). Figure 1 shows the historic exponential increase in the world's population and linear growth in the food supply.

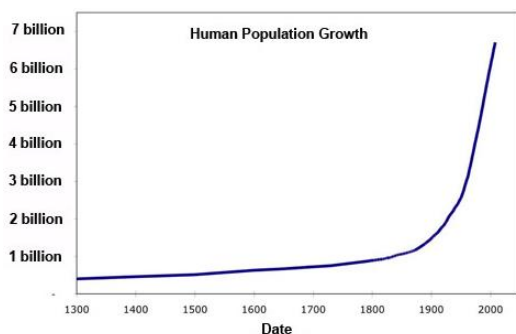


Figure 1. Historic population and food increase in the world over time (Emery, 2012)

Many countries around the globe are now importing cereals to fulfil the rising demands caused by the shortage of food supply. Unfortunately, agriculture has to face immense challenges due to the shortage of arable land resources, water resources, changing climatic conditions, and threats from pests and weeds (Lee *et al.*, 2010). Figure 2 is depicting this harsh reality by showing the net cereal import by developing nations since 1964, and the projected import in the year 2030.

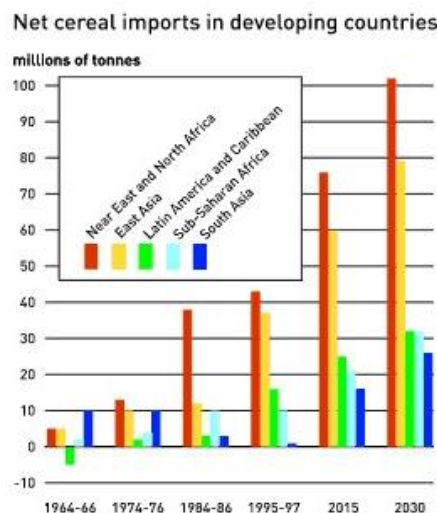


Figure 2. Existing and projected cereal import by developing nations (FAO, 2000).

Weeds can have a significant effect on reducing the average crop yield. The removal and extraction of weeds are done by spraying herbicides and using mechanical tools, but it requires considerable investment as you have to use it on the whole farm area. (Tyystjärvi *et al.*, 2011). For example, it is very expensive to manage wheat production in the initial stages due to weed (Ullah *et al.*, 2019). There is a growing need to control the number and quantity of herbicides sprayed on weeds to reduce economic and environmental losses.

These problems can be solved by detecting unwanted weed plants. Weed control aims to detect weeds from an image of the field and remove detected weeds using robotic rovers, which would ultimately improve the crop quality, increase crop yield, preserve soil nutrients, and reduce the cost of herbicide application. Thus, leading to a sustainable agricultural environment (Liu and Bruch, 2020). Various techniques have been used in recent times to remove unwanted weeds from crops. Mostly, in agricultural fields, weed control has been done by hand or by using different agricultural tools without using any automated procedures. Even now, these methods are still in practice in many small scale agricultural fields (Slaughter *et al.*, 2008; Saber *et al.*, 2015). Some Large scale farmers have adopted modern technologies to control weeds as the older techniques consume a great amount of time and require higher labor costs (Bakhshipour *et al.*, 2017). Weeds can be either uprooted through mechanical means or can be treated with a toxic substance that is used to demolish unwanted vegetation plants, known as the herbicide.

Traditional mechanical and chemical weeding methods can be enhanced using computing technology where a weed detection system can be mounted on the tractor or rover to detect and destroy weeds automatically. In artificial mechanical weed control methods, the system must identify the precise and exact location of crop and weed plants because any mistake can eliminate crop plants also (Dyrmann *et al.*, 2016). Chemical weed control methods can be automated using mobile robots. These robots move throughout the fields, detect weed plants in real-time, and then spray herbicides essentially on the weed plants that reduce the cost and time taken to apply herbicides evenly on the whole field. The automated weed control practices fall under the category of Precision Agriculture that aims to accurately manage agricultural farms while reducing the cost, time, and usage of resources (Tejeda and Castro, 2019). To detect weed plants accurately, this whole system requires precise information about the weed species, its growth stages, and plant density. The automated system can drastically decrease herbicide usage through precision agriculture. A 53% reduction in the application of herbicide to remove grass weeds in the wheat field was observed by Young *et al.* (2003), and a herbicide usage reduction of greater than 75% in the time-span of four years was shown by Gerhards and Christensen (2003) using Site-Specific Weed Management.

In current times, Computer Vision technologies are being used commercially in the field of horticulture and agriculture, effectively. Researchers have proposed various systems and methods for automatic identification of weed using Machine Vision techniques. Some of the effective techniques include Classification based on Chlorophyll Fluorescence (Tyystjärvi *et al.*, 2011), Fourier elliptic leaf shape analysis (Neto *et al.*, 2006), Nitrogen Diagnostic Model based on color and soya bean leaf texture (Wang, 2010), Inception v2 model based on GooLeNet (Tiwari *et al.*, 2019), texture features extraction through multi-scale scattering to successfully identify weed in high-density crops (Rasti *et al.*, 2019), and a decision tree-based technique that randomly chooses a subset of features associated with the objects in the image to reduce over-fitting and facilitate generalization (Peters *et al.*, 2007).

A typical machine learning model follows some basic series of steps, including pre-processing, background removal, noise reduction, feature detection, feature extraction, feature selection, and classification (Wang *et al.*, 2019). For noise reduction, various background elimination techniques like Basic Motion Detection (BMM), Gaussian Mixture Model (GMM), and Kernel Density Estimation (KDE) are used (Desai and Gandhi, 2014). Feature extraction and classification are the most important procedures as successful weed detection depends on the efficiency of these procedures. To recognize weeds from crop images, distinct features are first detected and then extracted. Primarily, features used to identify weeds are divided into 4 categories, including spectral features, spatial features, visual features, and morphological features. Color and spectral features are helpful only when there is a significant color difference between crop and weed plants. If this is not the case, then it is better to use shape features which involve the plant's morphology (Kazmi *et al.*, 2015).

## **OVERVIEW OF IMAGE PROCESSING METHODOLOGY**

This section provides an overview of generalized image processing technique adopted by researchers to build intelligent models to detect, identify, and extract objects from images. In most research papers, field images were captured and processed at real-time though some researches also involved laboratory images. The images are taken either through drone cameras or simply by placing the camera on a tripod stand. For real-time weed detection, the cameras are mounted over mobile robots that move across the field and capture field images.

These images are taken over months till the plants get mature by utilizing high-resolution cameras (Nandhini and Ravishankar, 2019). On the other hand, some researchers have trained their algorithms by downloading images of target crop and weed plants from online databases (Cheng and Matson, 2015). The sequence followed in these researches is

illustrated in Figure 3. The figure is depicting that at a first field or laboratory images are captured by using both infrared and RGB sensors. Then these images are preprocessed to eliminate background and noise. (Wang *et al.*, 2019).

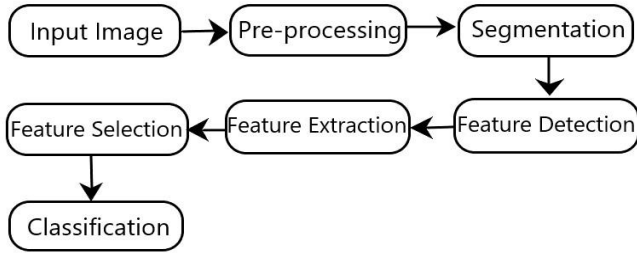


**Figure 3. The basic sequence of image processing**

The key benefit of pre-processing is to enhance image data by removing undesirable distortions and to improve such features that are crucial to train the algorithm (Nandhini and Ravishankar, 2019). In the next step, resizing and segmentation are carried out. Different procedures are used to segment the image and convert it from a 3-component RGB image to grayscale and binary image. This is done to reduce image data and to subtract the background from foreground objects. There is an eminent difference between the background soil and plant color in weed and crop images. So, the foreground and background pixels are easily separated using this technique (Wu *et al.*, 2011). The researchers have categorized the vegetation segmentation methods into threshold-based segmentation, color index-based segmentation, and learning-based segmentation (Hamuda *et al.*, 2017). However, according to a study presented by Wang *et al.* (2019), the color index-based method is also included in the threshold-based segmentation method.

After segmentation, the most crucial step in identifying weed from crop plants is feature detection and extraction. This review paper also summarizes the techniques to detect and extract features from crop and weed plant images. After feature extraction, feature selection is performed to acquire those salient features that provide the maximum information about the plant species. These selected features facilitate better classification of weed and crop plants.

### CATEGORIZATION OF IMAGE PROCESSING METHODS FOR WEED DETECTION

In this section, different weed detection algorithms have been presented that are classified based on their feature detection and extraction techniques. The efficiency of an algorithm depends upon the feature selection criteria to distinguish between crops and weeds. The details of the various algorithms specified in previous research works are given below.

**Spectral Features-Based Algorithms:** A model based on different reflectance properties of weeds, crops, and soil has

been explored by Vrindts *et al.* (2002). Their reflectance varies in Near-Infrared and visual wavelengths; therefore, one can easily use their reflection measurements in different wavelengths in order to discriminate them. The researchers have conducted experiments under both laboratory and field environments to find the potential of using spectral analysis for weed detection. They have considered sugar beet, maize along with 7 weed species for their experiment. The experiment was first performed in laboratory where the field of view of the camera to capture plant and soil images was 2cm. The recorded wavelength of spectra was from 400 to 2000 nm and a sampling interval of 0.5 nm. It was then reduced to 160 data points per spectrum by taking the average, i.e., one sample point per 10 nm. After collecting data, Statistical Analysis System (SAS) software was used. Stepwise Discriminant analysis STEPDISC was used to perform a stepwise discriminant analysis by backward elimination, forward selection, or stepwise selection of variables. Variables enter or leave a particular class on the basis of a covariance analysis and the significance level of the F-test. Then based on these selected variables, a discriminant model was developed for classification through Discriminant Analysis (DISCRIM) proc in SAS that considers the within class covariance. DISCRIM Proc uses the Bayes theorem to compute the probability of a data point belonging to a particular class. The mathematical equation is given by:

$$p(t|x) = \frac{q_t f_t(x)}{f(x)} \quad (1)$$

where  $x$  is the data point and  $t$  is the concerned class,  $q_t$  is the prior probability of  $x$  belonging to  $t$ ,  $f_t$  represents the density estimate at  $x$  from specific class  $t$  and  $f(x)$  is the unconditional density estimate. The experiment was also performed in field environment. For this purpose, the wavelength analyzed was in the range 400 to 900nm. Using Near Infra-Red (NIR) ratio, plant spectra were selected. Spectra ratio above 1.7 was analyzed as it denotes vegetation. The below value is that of soil. Here again, data reduction was performed by taking an average per 3 data points. Hence, the spectra produced as a result, has a resolution of 2.1 nm. Data below 484nm & above 814nm was considered to be the part of the noise. STEPDISC was used as in laboratory conditions. The DISCRIM proc was used to calculate and then test the discriminant models. Later the test dataset was also analyzed using these models. The researchers had also considered prior probabilities in the discriminant rule. At last, Jackknife test was implemented to do cross-validation. The results under Lab conditions using 7 wavelength ratios showed 85% correct classification of maize weed, 71% of sugar beet weed. In the Field environment (using 11 wavelength bands), 95% sugar beet test data, 15% maize, 84% sugar beet weed, 95% maize weed was classified correctly.

A hyperspectral mosaic camera with 25 bands was utilized by Gao *et al.* (2018) to get images for weed/maize classification. Each image was then cropped to 25 sub-images. Region of

interest (ROI) was extracted through roipoly function in Matlab 2016, and their calibrated reflectance was calculated for each band as:

$$R_{calibrated}(\lambda) = \frac{Raw(\lambda) - DC}{W(\lambda) - DC} (100\%) \quad (2)$$

Where  $Raw$  denotes the raw spectral images and  $R_{calibrated}$  is the calibrated reflectance.  $\lambda$  denotes the wavelength and  $DC$  shows the dark current value of the camera. The feature set was constructed by calculating 80 Ratio Vegetation Index  $RVI$  and Normalised Difference Vegetation Index  $NDVI$  using equations:

$$NDVI_{(\gamma_1, \gamma_2)} = \frac{NIR_{\gamma_1} - VB_{\gamma_2}}{NIR_{\gamma_1} + VB_{\gamma_2}} \quad (3)$$

$$RVI_{(\gamma_1, \gamma_2)} = \frac{NIR_{\gamma_1}}{VB_{\gamma_2}} \quad (4)$$

where  $NIR_{\gamma_1}$  shows one near the infra-red band and  $VB_{\gamma_2}$  represents one visual band. To select specific features that give the maximum information to facilitate classification, Principal Component Analysis (PCA) is applied. After that covariance, Eigenvectors and their related Eigenvalues of whole feature data were calculated. Those features with top 'k' Eigenvectors were sorted and selected to form a  $d \times k$  dimensional 'M' matrix. In the whole process, about one-third of data was not used in making a decision tree and was left to evaluate and calculate OOB (out-of-bag) errors. 'm' Decision trees were made from randomly selected 'n' features to predict new samples based on majority voting of these 'm' decision trees. 'M' matrix and 'n' (features to split decision trees) were the hyper-parameters. K-Nearest Neighbor (KNN) with Euclidean Distance (ED) was used in this process where  $k=5$ . At last F1 score was calculated for data evaluation using the formula:

$$F(i)_1 = 2 \times \frac{Precision \times Recall}{Precision + Recall} \quad (5)$$

Optimal Random Forest with 30 selected features gives better results than KNN. According to the results, the classification rate is 0.789 for *C. arvensis*, 0.691 for *Rumex*, 0.752 for *C. arvense*, and 1 for *Z.mays*.

An image processing technique to remove weed from lawn grass was proposed by Parra *et al.* (2019). The authors have collected field images using an Arduino module and a drone. The images were pre-processed, and the soil is removed based on colour-index by using the equation below.

$$S_r = G_b / R_b \quad (6)$$

Where  $S_r$  represents "soil removal",  $G_b$  accounts for the green band and  $R_b$  shows a red band. If the result of the above equation is greater than 0 then it is planted otherwise it is soil. Plant pixels have values greater than 0, and they are colored in green. On the other hand, soil pixels have values of 0, and they are colored in yellow. To distinguish two different types of weed, i.e., weed with bluish color and weed with yellowish color, two equations are used that are given below:

$$B_w = \left( \frac{B_b}{G_b} * R_b \right) * (G_b / R_b) \quad (7)$$

$$Y_w = \left( G_b * \frac{R_b}{B_b} \right) * (G_b / R_b) \quad (8)$$

Equation 7 and 8 were used to detect bluish weeds  $B_w$  and yellowish weeds  $Y_w$  from images by using the above raster combinations. In the resultant RGB picture, pixels having higher values and are joined with other higher value pixels after applying the above two equations are identified as weeds and are specified with red circles. Higher natural breaks, Jenks minimize within-group variance, considering only weeds to eliminate false positives. Different aggregation techniques using mean, median, and mode were used to smooth raster with cells of size 5 and 10. The study proposed that "median" aggregation with a cell size of 5 gives better results.

Another model was presented by Fawakherji *et al.* (2019) based on generating blobs from binary images and then classifying them into crops and weeds. A deep learning-based method is described for accurate weed/crop classification by a robot. The method was implemented using a sequence of 2 Convolutional Neural Networks Applied to the RGB images. Dataset consists of 500 sunflower images that are rotated at various angles, and the final dataset is of 2000 images. The soil was removed using a semantic segmentation network consisting of semantic Segmentation Network (SegNet) based on Visual Geometry Group (VGG-16) encoder and UNet based on VGG-16 decoder. VGG-16 encoder is modified by removing the last Fully Connected (FC) layers and tuning the remaining ones. Expanding decoder contains 4 convolutional layers, with each layer made up of batch normalization, a softmax pixel-wise classifier, and 4 up-sampling layers. A Dropout activation function has been used between the encoder and decoder. The segmentation performance had been improved by increasing the no. of input channels by a set of vegetation indices, including Excess Green (ExG), Normalized Difference Index (NDI), and Color Index of Vegetation Extraction (CIVE). To reduce the holes between foreground regions, dilation was applied to the binary mask as given in equation (9).

$$A \oplus B = \{z | (\hat{B})_z \cap A \neq \emptyset\} \quad (9)$$

Where  $z$  represents the displacements and  $(\hat{B})_z \cap A$  shows that  $\hat{B}$  and  $A$  are overlapped by  $z$  displacement. Blobs were extracted, a bounding box is drawn around the extracted blob in RGB image. For weed classification, training image dataset was passed through VGG-16 encoder with 13 Convolutional layers of 3x3 kernel size, max pooling layer with 2x2 kernel size, and Rectified Linear Unit (ReLU) as activation function which is given by the equation below.

$$ReLU(x) = \begin{cases} 1 & \text{if } x > 0 \\ 0 & \text{if } x \leq 0 \end{cases} \quad (10)$$

The evaluation procedure is done through mIOU, which is the ratio between the area of overlap and the area of union between the ground truth and the predicted areas. Results showed 90% accuracy, with 87% of crops that were correctly detected. 13% of the crops were detected as a weed due to overlapping. 32% of the soil was detected as a weed due to in-accuracies during dilation.

**Spatial Features-Based Algorithms:** In the research work presented by Wu *et al.* (2011), spatial features were utilized to identify weed in crop rows. After acquiring farm images, the RGB images were converted to greyscale as given by the formula:

$$f(i, j) = \begin{cases} 0 & 2G(i, j) < R(i, j) + B(i, j) \\ 255 & 2.5G(i, j) - R(i, j) - B(i, j) > 255 \\ 2.5G(i, j) - R(i, j) - B(i, j) & \text{Other} \end{cases} \quad (11)$$

where,  $R(i, j)$ ,  $G(i, j)$ ,  $B(i, j)$  are representing the value of 3-components of RGB image of the point  $(i, j)$ .  $f(i, j)$  is the grey value after changing the image to grey-scale. Then the grey image is segmented using a suitable threshold to separate soil. To extract inter-row, weed pixel histogram was used to set the centerline of crop rows and row edges through Robert's edge detector. To eliminate crop pixels, the sliding window moves over the image, and no. of black and white pixels are calculated. Distance thresholds  $D_{min}$  and  $D_{max}$  from crop centerline were set to identify crop pixels. After calculating the total no. of pixels and comparing it with the threshold, crop pixels are eliminated. Dilation and corrosion operations are applied to omit noise. Weed is then detected by dividing the image into small areas and calculating no. of pixels. The results of using this technique indicate a correct detection rate of 92-95% and a false detection rate of 3-5%.

A system based on two independent subsystems Fast Image Processing (FIP) and Robust Crop Row Detection (RCRD) was presented by Artizzu *et al.* (2011) for successful weed detection. Using spatial features to detect weed is not that popular as the weed grows in random patches, and so these features alone do not provide necessary information for successful classification. However, this concept is completely denied in the concerned research study. A camera was placed at the top of the tractor to capture field images. This paper focused on image processing in a real-time environment. The proposed model took 0.04 sec to process each frame, which means that a total of 25 frames were being processed in one second. For vegetation segmentation, a linear combination was used for RGB planes. The author evaluated two threshold methods, including Otsu's and mean pixel intensity, and then chose the latter one as it gave faster results. The equation (12) for threshold ( $T$ ) is given as follows:

$$T = \frac{\sum_{x=1}^N \sum_{y=1}^M (r \times R(x, y) + g \times G(x, y) + b \times B(x, y))}{M \times N} \quad (12)$$

Where ' $r$ ' represents red band with coefficient "- 0.884", ' $g$ ' denotes green band having coefficient "1.262", and ' $b$ ' shows the blue band with coefficient "- 0.311". After vegetation crop rows were computed using RCRD, which combined all binary frames with the help of AND operation in one image. The next step was to perform morphological operations to fill in image holes before region extraction in which crop rows comprised of 7 to 10 times larger region than weeds. Results obtained from this step were then processed by FIP. In this technique, images were first divided into horizontal sections.

The number of columns in one section is assigned as a vector that is given in equation (13):

$$V(x) = \sum_{x=strip\_start}^{strip\_end} I(x, y) \quad (13)$$

Where ' $I$ ' represents the image. As it was a binary image so the number of white pixels in each vector was considered and its width and height were compared to find crop and weed (Crop plants were having more height and width than weed plants). The systems were evaluated using the mean percentage of correctly labelled crop and weed pixels. According to the results given, 80% of crops and 95% of weed were correctly classified with 1% false negative.

**Morphological Features-Based Algorithms:** A near-ground image processing techniques to detect broad-leaved weeds in cereal crops was discussed by Pérez *et al.* (2000). Images were first converted to a greyscale through the NDI. After applying NDI, the resultant image is in range -1 to +1. So, to convert it to range 0-255, the authors have added +1 and multiply with 128. In the next step, grayscale images were transformed to binary using a bimodal histogram (left mode for soil and right mode for plants). Two thresholds were defined  $T_H$  (high threshold) and (low threshold) using a bimodal histogram. The threshold  $T_H$  (on the right of histogram valley) gave good results and generated a "seed image". Images with threshold  $T_L$  had some plants segmented with background objects, so the image was called "limit image". Dilation was applied to the seed image with the limit image as the dilation limit. The dilation process was repeated several times until pixels were no more added to the seed image. In this way, the final segmented image was generated. The position of crop rows was determined through histogram by summing up crop pixels in a column. Then a low pass filter was applied, and an absolute maximum was calculated. Plants outside rows were labelled as a weed. For intra-row plants, shape analysis was done. Feature distinctiveness was computed using the Fisher ratio. In this way, only those features were selected that provide useful information for classification and help to reduce response time and classification complexity. Feature distinctiveness or the extent of overlapping between the two classes of crop and weed was calculated using equation (14).

$$V = \left| \frac{\bar{x}_w - \bar{x}_c}{\sigma_w^2 + \sigma_c^2} \right| \quad (14)$$

where  $V$  represents the normalized variance of distance between the mean points of both classes,  $\bar{x}_w$  shows mean of class weed,  $\bar{x}_c$  denotes mean of crop class, and  $\sigma_w^2 + \sigma_c^2$  denotes the sum of squared distances between crop and weed. Selected features were normal axis relation, distance to crop row, first invariant central moment, major axis length, the ratio of the perimeter, and major axis length squared to area ratio and heuristic index to determine weed type obtained after dilation and erosion. In the heuristic index, the decision was made based on the fact that most weeds were dicotyledons. The values of the resultant feature set were rescaled in the range 0-1. The train/test split was based on the

ratio 70:30, where 70% of the images constitute a training dataset, and 30% of images were part of the test dataset. Two pattern recognition methods were used: Bayes rule (calculates the probability of a feature belonging to some class) and KNN. Multiedit was used to clean boundaries b/w classes by clearing ambiguities, and after that, condensing tech (CNN) was applied (to lower the no. of prototypes). For crop, Bayes resulted in 89.7% and KNN in 89% correct detection. For weed, Bayes has 74.5%, and KNN has a 79.2% detection rate. Another smart technique for weed identification that is based on “active shape modelling” was presented by Swain *et al.* (2011). This technique utilizes the biological morphology of plants to find distinct features. A Complementary metal-oxide-semiconductor (CMOS) camera was used to acquire color images of the nightshade. Each training image of the black nightshade was aligned by rotating, scaling, and translating by using standard MATLAB (Matrix Laboratory) commands. Then the RGB images were converted to binary images using an Excess Green Index (EGI) that caused the segmentation of plants and soil. It is given by equation (15) where  $G$ ,  $B$  and  $R$  exhibit green, blue and red respectively.

$$EGI = \frac{G \times 3}{G+B+R} \quad (15)$$

Then individual leaves in images were analyzed, and their continuous edges were detected using Sobel edge detection. A single 3 x 3 matrix of image filter identifies the edge using Automated Active Shape Matching (AASM) technique. This operation of “active shape matching” was supported by LTI-lib. The next step was to develop a point distribution model of each leaf. This process is carried out by manually registering the edges in MATLAB. Virtual landmark points were used to mark the edges of each leaf. The coordinates of landmark points belonging to all manually registered 32 images were utilized to construct a “Mean Model”. The mean model  $\bar{X}$  was estimated using the following equation:

$$\bar{X} = \frac{1}{N} \sum_{i=0}^N X_i \quad (16)$$

Now a “mode of variation” is a way in which landmark points change as the shape changes. The deviation of every training shape in comparison with the mean model is calculated. Then PCA used to evaluate the mode of variations via a covariance matrix denoted by ‘ $S$ ’ featuring the landmark points.

$$S = \frac{1}{N} \sum_{i=0}^N (X_i - \bar{X}) (X_i - \bar{X})^T \quad (17)$$

The mode of variation given by the Principal axes of an ellipsoid which is given as:

$$SP_k = \lambda_k P_k \quad (18)$$

where  $k$  is given as  $(1, 2, \dots, 2n)$ ,  $S$  refers to the unit eigenvectors, mode of variation is given by  $P_k$  and  $k^{\text{th}}$  eigenvalue by  $\lambda_k$ . Those Eigenvectors in the covariance matrix that comprise of the largest Eigenvalues represent the longest axes of ellipsoid. The derivative profile of a new image is to be compared with the Mean Model and see if it has got the highest resemblance. At last, the leaf shapes, identified as weed or nightshade, were analyzed individually

to find the accuracy of the system. Accuracy for the 2-leaf stage is 90%, and for the 3-leaf stage, it is 100%. This technique took only 0.053 sec for target identification.

A classification technique based on area feature was described by Hlaing and Khaing (2014). In this work, RGB images were first converted to greyscale using the below equation:

$$ExG(x, y) = 2g - r - b \quad (19)$$

where  $r = \frac{R}{R+G+B}$ ,  $g = \frac{G}{R+G+B}$ ,  $b = \frac{B}{R+G+B}$  and  $ExG$  is the converted grey-scale image. Noise reduction was done using Median filtering. The threshold for binarization was calculated using the Otsu method.

$$g(x, y) = \begin{cases} P, & |G - R| > T \text{ and } |G - B| > T \\ Bg, & \text{Otherwise} \end{cases} \quad (20)$$

where  $g(x, y)$  indicates binarized image,  $R$ ,  $G$ ,  $B$  represents the red, green, and blue component pixel values and  $T$  denotes the threshold. For conversion to a binary image, the distances between red-green pixels and blue-green pixels were computed and then compared with the set threshold. After that, the watershed segmentation method was used to divide the binarized image into different regions. In this method, the author found gradient magnitude by applying the Sobel operator on the binary image. The gradient magnitude was further used to compute the watershed transform, which in turn divide the image into different regions. Pixels were labelled based on 8-connectivity. The remaining pixels were discarded. The areas of the individual objects were calculated according to the equation.

$$M(m, n) = \frac{1}{j^m k^n} \sum_{j=1}^J \sum_{k=1}^K (x_j)^m (y_k)^n F(j, k) \quad (21)$$

where  $F(j, k)$  is the binarized image,  $x_j$  and  $y_k$  are the scaled pixel coordinates. The desired image points were calculated by:

$$x_j = j + 1/2 \quad (22)$$

$$y_k = k + 1/2 \quad (23)$$

The selected threshold  $T$  in this work is 6000 and was given by equation (24) where  $w$  represents weed and  $C$  represents crop.

$$I = \begin{cases} w, & \text{area} < T \\ C, & \text{area} \geq T \end{cases} \quad (24)$$

At the end error rate was also calculated. Through this method, the maximum weed misclassification rate turned out to be 33.3%.

A weed detection technique based on area features extracted from weed and crop plants is explained by Villa *et al.* (2016). In Eq. (25) the green component ( $I_{G,S}$ ) of RGB image was utilized to segment green and vegetative part and to remove soil (background) from images.

$$I_{Plant}(X_{Pixel}, Y_{Pixel}) = I_{G,S} \quad (25)$$

$$I_{Plant}(X_{Pixel}, Y_{Pixel}, G) - I_{Gray}(X_{Pixel}, Y_{Pixel}) \quad (26)$$

where  $I_{Plant}(X_{Pixel}, Y_{Pixel}, G)$  denotes the green component of plant image, and  $I_{Gray}(X_{Pixel}, Y_{Pixel})$  denotes the grayscale image. Images were first converted to grayscale, and then the

green value components were subtracted from grey components. To remove noise, median filtering was used with a 3x3 filter mask as it retains edges while eliminating noise. Next is to separate objects of interest using a threshold. To estimate the threshold ‘ $t$ ’, Otsu’s method was used and then an appropriate threshold is selected using histograms. Following equation is used in this process.

$$I_{bin}(x, y) = \begin{cases} 0, & I_{median}(x, y) < t \\ 1, & I_{median}(x, y) \geq t \end{cases} \quad (27)$$

where  $I_{median}$  shows a filtered image. If the pixel intensity of the filtered image is less than threshold  $t$  then the value is converted to 0. On the contrary, if the pixel values are greater than or equal to the threshold then they were assigned the value 1. To fill image holes, morphological operations were carried out with 4-8 neighbourhood connectivity pixels. Its equation is given as:

$$F_{mark}(x, y) = \begin{cases} 1 - I_{source}(x, y), & (x, y \text{ is on the border of } I_{source}) \\ 0, & \text{otherwise} \end{cases} \quad (28)$$

$$H_k = (H_{k-1} \otimes B) \cap G \quad (29)$$

where  $B$  is the ones matrix of size 3x3,  $H_k$  is the resultant binary image. In the next step, pixels were labelled using a 4-neighbour connectivity algorithm. In the classification phase, the area was calculated by counting pixels and then setting the threshold for weed. At last, the algorithm was evaluated done through Specificity, Sensitivity, Positive and negative predictive value. Results showed that the algorithm had a sensitivity of 0.90 that is good, a specificity value close to 1 that shows correct crop classification, a positive predictive value greater than 80%, and false negatives of about 30%.

Another area thresholding method to identify weed in laboratory environment was used by Vikhram *et al.* (2018). In this paper, images were taken at regular interims, and then herbicide was sprayed specifically on weed. To capture images, a Raspberry Pi camera was used, mounted on a robotic arm, and at a ground distance of about 40cm. Then the images are converted to grayscale by using `cv2.cvtColor()` function of OpenCV. The coefficient used in `cv2.cvtColor()` function for RGB to Grayscale conversion are given as:

$$Y = 0.299 R + 0.587 G + 0.114 B \quad (30)$$

After that the author masked image to green color with a masking range of (36,0,0) (86, 255, 255) in OpenCV via `cv2.inRange()` function. The mathematical equation for applying `cv2.inRange` to an input array of single dimension is given by equation (31).

$$dst(I) = lowerb(I)_0 \leq src(I)_0 \leq upperb(I)_0 \quad (31)$$

Where *lowerb* and *upperb* represent the lower and upper boundary of the range and *src* refers to the initial input array. The nearness of yields for the Region of Interest was calculated by performing morphological thresholding, dilation, and erosion. Then to differentiate between weed and crops, their no. of pixels were calculated. A threshold value was set based on the number of pixels, which is more for weed as they have broader leaves. Multiple weed images were

processed to get the threshold value. The process is to calculate the number of pixels of the input image. If it is greater than the threshold value set initially, then the image was considered a weed and vice versa. The threshold value set after processing multiple images is around 90000. A motor driver, namely L293D IC was utilized in this paper to interface the two motors, i.e., pump motors and wheel motors with Raspberry-Pi. All the processing was done using Python and Open CV. Results after conducting this experiment showed that all the weed plants were successfully distinguished. Conditions, where the weed plants were found in vast groups, showed some false detection of Ragiplants (*E.coracana*) being identified as weeds.

A study based on analyzing blobs to extract shape features was discussed by Murawwat *et al.* (2018). The proposed system was made to detect weed in carrot crops. The work is divided into several steps. In the first step, input sample images were loaded in which all the data was collected in a single set. Then a try-catch loop was used to get one image at a time. To reduce image data, the image size was reduced by 50%. Then the image was converted to greyscale by just considering the “green” component of the RGB image using equation (32).

$$G = X(:, :, 2) \quad (32)$$

Where  $G$  represents the Green component of RGB image ‘ $X$ ’. This would get all the pixels of the second array of an RGB image that constitutes the green color band. A threshold  $T$  was set as 10% of the greyscale image. This threshold was used for binarization. The plant pixels were identified using the below equation.

$$G > T \quad (33)$$

If the above condition is satisfied, then the pixel is said to be a vegetation pixel. After that, blob analysis was done in which blobs were generated based on the length and centroid of crop ad weed leaves. At last, a bounding box pointed out the weed if present, and the procedure repeated until all images were processed. Samples with maximum crop or weed were successfully classified by Support Vector Machine (SVM). Samples with no overlapping between crop and weed leaves were identified with 100% accuracy, and those with few overlapping scenarios also showed 90% accuracy. Unfortunately, the algorithm did not perform well in samples with considerable overlapping of weed and crop leaves.

An algorithm based on detecting weed through plant shape and edge frequency was elaborated by Kaarthik and Vivek (2018). Based on these two features, weeds were categorized into three main types including those with narrower leaves (edge frequency of these weeds was less as compared to others), those with leaves arranged in clusters (these leaves have relatively medium edge frequencies), and then those with comparatively wider leaves (These are the weeds with high edge frequencies). In the first step, image segmentation was done by setting the threshold using Otsu’s method, and then that threshold was used to create a binary image. After

doing image segmentation, a Rank filter (median filter) was used to remove noise from images to avoid any misclassification later on. The sliding window  $W_i$  used to extract the median of pixels inside the window is given as:

$$W_i = \{X_i + r : r \in W\} \quad (34)$$

where ‘ $i$ ’ identifies the starting position of the window. The mathematical equation for a standard median filter is given by equation (35).

$$Y_i = \text{med}\{W_i\} = \text{med}\{X_i + r : r \in W\} \quad (35)$$

where  $X_i$  and  $Y_i$  denotes input and output at the  $i^{\text{th}}$  position. The algorithm was designed to identify weeds in the corn crop. The corn plants had narrower leaves in contrast with the weed leaves, and so the corn crop has less edge frequency. So, in this work, a relatively high threshold value of 500 was set to identify weeds. Two loop structures were used. The first loop was “IF loop” used to recognize the values of threshold. The second loop was “FOR loop” used to find if the threshold value is less than the edge frequency of the plant. If the plant’s edge frequency is greater than the threshold, then it is identified as a weed. The plants’ pixels are classified into their respective classes by using K-means clustering. In this process, the objects are classified based on the distance between the extracted features. The proposed algorithm can be used with an automatic sprayer or robotic hand.

**Visual Features-Based Algorithms:** The algorithm proposed by Pulido *et al.* (2017) was used to detect weed in vegetable crops through SVM classification. GLCM (Grey level co-occurrence matrix) texture features were used to distinguish between crops and weeds. A GLCM was computed using 10 texture features, including contrast, correlation, autocorrelation, homogeneity, energy, dissimilarity cluster shade, variance, and difference variance. All these ten features were calculated using formulas. The GLCM was defined mathematically as:

$$C_{\Delta x, \Delta y}(i, j) = \begin{cases} 1, & \text{If } I(p, q) = i \text{ and } I(p + \Delta x, q + \Delta y) = j \\ 0, & \text{otherwise} \end{cases} \quad (36)$$

where  $C$  denotes a co-occurrence matrix for image ‘ $I$ ’ of size  $m \times n$  having parameters  $\Delta x$  and  $\Delta y$ . For training purposes, the images were first labelled manually. These images were divided into grids before extracting features. After feature extraction, PCA was applied to reduce dimensions by keeping only those feature variables showing the maximum variance (with greater Eigenvalues and greater length of principle axis component) for the two categories. It was given by:

$$Y = \alpha X \quad (37)$$

Where  $\alpha$  represents principal components and  $X$  shows the covariance matrix. After this step, SVM was used to differentiate the two classes with a separating hyperplane is given in equation (38).

$$wx + b = 0 \quad (38)$$

Where the variable ‘ $w$ ’ is normal to the hyperplane, and  $b/w$  is the perpendicular distance from hyperplane to the origin. The main purpose was to increase the distance between

support vectors and the hyperplane by maximizing the margin. Equation (39) and (40) were used for this purpose which is given below:

$$\text{Min: } w^2 = \phi(w, b) \quad (39)$$

$$\text{Subject to: } y_i[w, x + b] - 1 \geq 0 \quad (40)$$

The Radial basis function (RBF) kernel was used for classification through SVM. Then the next step was to optimize the algorithm. This was done by applying 10-fold cross-validation. At last, data was evaluated by finding the sensitivity, specificity, positive, and negative predictive values of data. Results showed that the proposed algorithm had high values (greater than 90%) for both specificity and sensitivity.

The research work presented by Rehman *et al.* (2019) focused on the classification and detection of golden rod (GR) weed in the wide blueberry (WBB) crop. This crop usually requires heavy application of herbicides, and so there was a crucial need to develop an automatic weed detection system that can be implemented in the sprayer robot to target weed specifically for herbicides. The cameras were mounted on the robot vehicle and were placed 0.18m in front of spray nozzles. This, in turn, provides greater buffer distance and extra time for processing images. The whole software was developed in C-sharp using visual studio 2010. An area of interest of 768×128 pixels was captured from the complete frame (1280×1024) of the image. This was done to minimize radial lens distortion. The original image color space was changed to Hue-Saturation-Intensity (HSI) color plane used to construct the three-colour co-occurrence matrix (CCM). These were developed by calculating the relative frequency between 2 pixels that are separated at orientation angle ( $\Theta$ ) by a distance-vector ( $d$ ) and with an intensity level of 256. All the CCMs were then normalized through the equation:

$$p(i, j) = \frac{P(i, j, 1, 0)}{\sum_{i=0}^{G-1} \sum_{j=0}^{G-1} P(i, j, 1, 0)} \quad (41)$$

Where  $p(i, j)$  is the normalized color co-occurrence matrix, and  $P(i, j, 1, 0)$  represents the relative co-occurrence frequencies of intensities  $i$  and  $j$  with ‘0’ degree angular orientation and ‘1’ distance vector. Thirteen textural features were extracted from each H, S, and I matrix which results in generating 39 features from every single image. This process generated training and test datasets in comma-separated values (CSV) format. Then the most discriminating features were selected from a set of 39 features using the SAS STEPDISC proc. Forward-selection and backward elimination were chosen for feature selection with a threshold level of 0.0015 for F-to-enter and 0.0010 for F-to-remove. The features of data models DM-H<sub>SD</sub> (STEPDISC Data Model for Hue), DM-S<sub>SD</sub> (STEPDISC Data Model for Saturation), and DM-I<sub>SD</sub> (STEPDISC Data Model for Intensity) were reduced by removing other planes’ CCMs followed by feature reduction procedure. 3 data models (DM-HS<sub>SD</sub>, DM-HI<sub>SD</sub>, and DM-SI<sub>SD</sub>) were developed by reducing features from all the possible combinations belonging to two

color planes. The final model (DM-HIS<sub>SD</sub>) was extracted by reducing the features of all 3 color planes. This is done to select features with the highest classification accuracy and minimum computational load. One single sprayer nozzle is controlled by 3 Decision units generated from 3-unit images.

$$Decision\ Unit = \begin{cases} 1, & \text{if } GR > WBB \\ 0, & \text{else} \end{cases} \quad (42)$$

Outputs of all the classifying models were compared by using 'if-else' logic for the GR and WBB for each image. The result was computed using equation 42 and stored in a decision unit array. 7 Data Models were selected to develop classifiers by using SAS PROC DISCRIM procedure that has provided coefficients related to each feature. The resultant quadratic classifiers were based on squared Mahalanobis Distance and within-group covariance matrices. This process of calculating coefficients has been repeated for all models.

$$d_{GR}^2(X^*) = (x - m_{GR})^T V_{GR}^{-1} (x - m_{GR}) \quad (43)$$

$$S_k(X^*) = c_k + b_{k1}X_1 + b_{k2}X_2 + \dots + b_{kp}X_p \quad (44)$$

Equation (43) is for squared MD where  $x$  is a vector which contains quantitative values of all features of  $X^*$ . Equation (44) shows a classification score of  $X^*$ . Its performance evaluation was done by calculating Sensitivity, Accuracy, Specificity, and FNR. 70% of data is included in training and 30% invalidation. DM-HIS<sub>SD</sub> data model achieved the highest accuracy of 94.98% for training and 93.80% for testing datasets. Also, the accuracies of all linear DMs for test data were less as compared to their respective quadratic models. Results of experiments at lab-scale suggested the selection of DM-HSI<sub>SD</sub> (STEPDISC data model for Hue-Saturation-Intensity) and at field scale for selection of quadratic classifier to target the weed spots in real-time.

**Algorithms Based on Multiple Features:** In addition to the above criteria used by algorithms to detect and extract key features for classification, some image processing algorithms use both shape and color features to give optimal results, especially in a real-time classification environment. Mostly, it is applied in cases where both inter-row and intra-row weed is detected. Normally crop plants are sown at regular intervals and in specific rows. So, plants outside the rows are classified as a weed. This approach of weed identification was proposed by Pérez *et al.* (2000) and Sujaritha *et al.* (2017).

The use of agricultural mobile robots for successful mechanical weed control was illustrated by Åstrand and Baerveldt (2002). This paper mentioned an automatic robot that utilizes two vision systems. One is the grey level vision system, and the other one is the color-based vision system. The first one is for row following, and the second one is for within row crop (sugarbeet) detection. These vision systems were implemented in the autonomous mobile robot, which in turn detects and then mechanically eradicates the weed plants. Normally, the weed detection systems used to detect 2-5 different species, but the presented system was designed for high weed pressure, i.e., it can detect up to 12 different species of crop and weed plants. A forward-looking grayscale camera

mounted on the machine with a NIR filter through which it could capture the high-contrast image. Then an opening operation is carried out on the image to reduce the effect of diff lights in an outdoor environment. Image opening features erosion operation followed by dilation and is given as:

$$f \circ s = (f \ominus s) \oplus s \quad (45)$$

Where  $f$  denotes the image,  $s$  refers to the structuring element  $f \ominus s$  indicates erosion and  $\oplus s$  represents dilation operation. The resultant image is subtracted from the original image to produce a grayscale image. The advantage of using NIR is that it gives a high-contrast image so that the vegetation seems bright and the soil appears dark. To detect crop rows, Hough Transform is used as it is robust in finding lines, especially when the lines are extended in the whole image. The lines in the image are given by equation (46).

$$y_i = ax_i + b \quad (46)$$

where  $x_i, y_i$  denotes the edge point and the above equation specifies the line passing through that valid edge point.  $a$  and  $b$  are the coefficients that were found by Hough Transform. Instead of a single line, the researchers modelled a plant row using a rectangular box containing adjacent lines. The box has a width equal to the plant's width and an unlimited length throughout the image. All the cop pixels become part of these lines and the rest is considered noise in the binary image. The author finds a linear relationship between the pixel offset to row 's' and pixel angle to row 'α' via Perspective Transformation which is given as:

$$A\alpha + Bs + C \quad (47)$$

Where  $A, B,$  and  $C$  are constant and are functions of the pixel  $(x_i, y_i)$ . Next to detect plants within rows, firstly a histogram thresholding method is applied for binarization and an appropriate threshold was calculated using Otsu's method. Then to remove noise, morphological opening and closing performed on the resultant image proceeded by a flood-fill operation. Six color features (mean and standard deviation for the red, green, and blue component), seven shape features (perimeter, elongation, area, solidity), and six moment-based features were extracted. These features were in turn, used to classify weeds and sugar beets using k-nearest neighbour and Euclidean distance (for calculating the nearest neighbour). A simple linear rescaling step is used to rescale feature values so that these transformed feature variables had 0 mean and Unit S.D (standard deviation). Results showed that by using KNN for all the 19 features, the system achieved a 97% classification rate. The row recognition system had an error standard deviation ranging from 0.6cm to 1.2cm. When implemented in a mobile robot, its offset error was about  $\pm 2$ cm.

The technique proposed by Ishak *et al.* (2008) enables automatic classification of broad and narrow weed to control weed growth and to limit the use of herbicides sprayed in an oil palm plantation, Malaysia. Feature vectors are extracted by using a combination of Gabor filter and Fast Fourier Transform (FFT) along with an SVM classifier. Firstly,

images were resized and then converted to grayscale using MExG. Then Gabor filters of different orientation pair (e.g., 0°, 90°) are applied to the resultant image for texture analysis. After that FFT was implemented, and the difference of their output is taken as “diffFFT gabor” feature, and the task is repeated for another pair. Then the two species were separated based on the above feature vector using an SVM separating hyperplane. The researcher used an RBF kernel function with width  $\sigma$  as:

$$K(x, y) = \exp\left(-\frac{\|x-y\|^2}{2\sigma^2}\right) \quad (48)$$

The optimization function used is given in equation (49).

$$W(\alpha) = \sum_{i=1}^M \alpha_i - \frac{1}{2} \sum_{i=1}^M \sum_{j=1}^M \alpha_i \alpha_j y_i y_j K(x_i, x_j) \quad (49)$$

$$\sum_{i=1}^M \alpha_i y_i = 0, \quad 0 \leq \alpha_i \leq C \quad (50)$$

Where  $\alpha$  is Lagrange multiplier,  $y$  is a class label and  $x$  is a set of the feature vector. Parameter  $C=10$  is selected. Results showed that with parameter  $C$  other than 10, the accuracy of both broad and narrow class is less than 90 with  $C=10$ , accuracy is 100.

The research work presented by Kodagoda *et al.* (2008) utilized various visual cues related to color and texture, and then the cues which gave the best result were automatically selected by an unsupervised algorithm. The main purpose of detecting weed in wheat is to increase wheat production (Hameed and Amin, 2018). Images of Bidens, wheat, and Lolium were taken under laboratory conditions. A simple color-based classification procedure is used for the detection of plant and soil. Various visual cues (hue, saturation, texture, NIR measured through Gabor filter.) and their combination were calculated for foreground pixels. The calculated cues and their combinations were classified into several numbers of clusters based on the k-means clustering algorithm. The mathematical formula for k-means is given in equation (51).

$$J = \sum_{j=1}^k \sum_{i=1}^n \|x_i^{(j)} - c_j\|^2 \quad (51)$$

where  $k$  represents the no. of clusters,  $n$  shows the no. of cases,  $x_i$  denotes the  $i$ th case and  $c_j$  represents the centroid for cluster  $j$ .  $\|x_i^{(j)} - c_j\|^2$  gives the distance function. Then Mahalanobis Distance (MD) was calculated. The cues and their combinations with greater MD were chosen. The mathematical representation of Mahalanobis distance is given by:

$$D = \sqrt{(x - m)^T \cdot C^{-1} \cdot (x - m)} \quad (52)$$

Where  $D$  represents the Mahalanobis distance,  $x$  is the concerned vector,  $m$  represents mean of all independent variables, and  $C^{-1}$  is the inverse covariance matrix. A Probabilistic model based on chosen features was established. Then a classification algorithm was made, and pixels were categorized (Pixels with  $MD < 1$  were given a value of 1, and others were given a value  $1/MD$ ). To improve the connectivity of high probability pixels, morphological operations were carried out. Results showed that a combination of saturation and has given separable clusters.

With Bidens, wheat has 77%, and Bidens has 97% detection rate. When wheat experimented with Lolium then Lolium got 26% while wheat got 85% detection rate.

A research work based on a combination of two feature categories including area feature and moment of order features was presented by Masuda *et al.* (2010). In the very first step, pixels with rice ears were separated using equation (53) with  $G$ ,  $R$ , and  $B$  representing green, red and blue image pixels:

$$G > 150 \wedge G - R < 30 \wedge G - B > 80 \quad (53)$$

Extraction of rice ears is followed by calculating area and moment features separately for each pixel using the given equation.

$$A = 255 \times \frac{N_{ear}}{W_{width} \times W_{height}} \quad (54)$$

Where  $W_{height}$  and  $W_{width}$  are the height and width of the window, and the nominator represents the rice ear extracted before. The moment of order calculated for a pixel is shown in equation (55).

$$M_{m,n} = 225 \times \frac{\sum_{x,y} (x-cgx)^m (y-cgy)^n I(x,y)}{\max[\sum_{x,y} (x-cgx)^m (y-cgy)^n I(x,y)]} \quad (55)$$

where  $cgx$  and  $cgy$  were coordinates of pixels' centre of gravity. Then to discriminate crop and weed, each image was divided into sections of 40x40 pixels. Following criteria were used for the identification of rice ears.

For area:  $20 < \max(A) < 90$

For 3<sup>rd</sup> moment order:  $SD(M_{3,0}) > 15$

Resultant images showed better performance by third-moment order, so this feature was selected to discriminate rice ears from weed.

An algorithm designed to automate the process of weed detection and herbicide application on site-specific locations by using color, shape and moment invariant features was discussed by Ahmed *et al.* (2012). The images utilized in this paper were captured from Chili (*Capsicum frutescens* L.) field along with the other 5 weed species. The camera was set with a ground-camera distance of about 40cm. Image resolution was set to 1200x768 pixels. At first, images were pre-processed by converting them to grayscale. This is done by only considering the green component 'G' value. Then a threshold was calculated for 'G'. Those pixels with G value greater than the set threshold 'T' were considered plants, and the remaining pixels were part of the soil. The global thresholding technique was used for binarization of the grayscale images. The next step in pre-processing was to remove thin protrusions and to make the image contours smooth. This was done by performing a morphological opening in which an erosion operation is done after dilation. Morphological closing was applied by performing dilation after an erosion operation had been applied to the image to eliminate small holes. Fourteen features were extracted in total from each image. Color features (r, g, b) were extracted using equations 56, 57 and 58 respectively.

$$r = \frac{R}{R+G+B} \quad (56)$$

$$g = \frac{G}{R+G+B} \quad (57)$$

$$b = \frac{B}{R+G+B} \quad (58)$$

where  $R$ ,  $G$ ,  $B$  refers to the red, green and blue bands in an image. Through this, the color becomes consistent with various light conditions. After that shape features were extracted including Elongatedness, Form factor, Solidity and Complexity using equations (59), (60), (61) and (62).

$$\text{Form factor} = 4\pi \frac{\text{area}}{\text{perimeter}^2} \quad (59)$$

$$\text{Elongatedness} = \frac{\text{area}}{\text{thickness}^2} \quad (60)$$

$$\text{Convexity} = \frac{\text{convex\_perimeter}}{\text{perimeter}} \quad (61)$$

$$\text{Solidity} = \frac{\text{area}}{\text{convex\_area}} \quad (62)$$

Where  $area$  refers to the no. of the pixel with value 1 in a binary image,  $perimeter$  denotes the boundary pixels,  $convex\_area$  is the smallest convex hull area covering all plant pixels, and  $convex\_perimeter$  is the boundary pixels of that convex hull. After color and shape features, moment invariant features were also extracted. These are called ‘‘Hu moments’’ and contains second and third-order moments given by:

$$\varphi_1 = \eta_{2,0} + \eta_{0,2} \quad (63)$$

$$\varphi_2 = (\eta_{2,0} + \eta_{0,2})^2 + 4\eta_{1,1}^2 \quad (64)$$

$$\varphi_3 = (\eta_{3,0} - 3\eta_{1,2})^2 + (\eta_{0,3} - 3\eta_{2,1})^2 \quad (65)$$

$$\varphi_4 = (\eta_{3,0} + \eta_{1,2})^2 + (\eta_{0,3} + \eta_{2,1})^2 \quad (66)$$

Where  $\varphi_1$  and  $\varphi_2$  denotes the second-order and  $\varphi_3$  and  $\varphi_4$  belong to third-order Hu-moments or moment invariant features. The best thing is that these moments of invariants are invariant to reflection and rotation, and so they give better results when it comes to detecting weed in a real-time environment under varying light and reflection conditions. The training data was then utilized to generate a classification model through SVM. Two approaches can be used for multiclass classification. The first one is ‘‘one against rest,’’ and the other one is ‘‘several two-class’’ approach. The approach selected in the presented paper was the ‘‘one-against-rest’’ approach. After training, the model was used to predict the classes of test data images based on the above-extracted features. The dataset was normalized before using it. LIBSVM 2.91 library was utilized to implement this method. The kernel used in this process was RBF kernel and its function is illustrated in equation (67).

$$K(x_i, x_j) = \exp(-\gamma \|x_i - x_j\|^2), \gamma > 0 \quad (67)$$

Where  $x_i, x_j$  are the feature vectors for the  $n$ -dimensional matrix and  $\|x_i - x_j\|^2$  is given by equation 68.

$$\|x_i - x_j\|^2 = (x_i - x_j)^t (x_i - x_j) \quad (68)$$

After repeating experiments, the C-parameter and gamma ( $\gamma$ ) selected for SVM was 1.00 and  $1/n$  respectively. Optimal feature selection is done through the forward selection and backward elimination. Ten-fold cross-validation was used in testing. The accuracy of the proposed method using all the 14

features was 95.9%. No weeds were misclassified. The classification rate is 96.4% using forward selection, with 8 features, 96.9% using backward elimination with 9 features, and 97.3% using Stepwise feature selection with 9 features. Another algorithm discussed by Cheng and Matson (2015) was based on color and texture features to automate the process of detecting weeds from rice. The input images containing rice and weed plants were of size 1125x1500. The dataset was obtained from an online source. Each image is then divided into sub-regions of size 480 x 360 from the top left corner to the bottom right. In the next step, the Harris corner detection algorithm was applied. This algorithm marked the region of interest (ROI) in each sub-image, including the tips of roots, leaves, and branches. Mathematically it is given by the following equations.

$$E(u, v) = (u, v)M(u, v)^T \quad (69)$$

where  $u$  and  $v$  represent the coordinates of the window, and  $T$  indicates the transpose of  $2 \times 2$  matrix  $M$  which is derived from the image as:

$$M = \sum_{x,y} w(x, y) \begin{bmatrix} I_x^2 & I_x I_y \\ I_x I_y & I_y^2 \end{bmatrix} \quad (70)$$

where  $I$  denotes the image with  $(x, y)$  coordinates. A  $40 \times 40$  window was used to extract color features, including mean red, mean green, mean blue, std. red, std. green, and std. blue. Then texture features were also extracted using histograms like mean of the histogram, its variance, skewness, and flatness. While keeping Harris corner pixel at the centre of the window. To consider a pixel position, a co-occurrence matrix was also used to extract features like Contrast, correlation, and uniformity. Then information gain for each feature is calculated. As a result, three features were removed with ‘0’ Information Gain. These features and ground truth (based on manual labelling) are used to train Machine Learning algorithms like SVM, Decision tree, and neural network. The whole data was divided into 10 equal parts. Each part has a ratio of 9:1 for training and testing data, respectively. This ratio was achieved by the 10-fold Cross-Validation, and the procedure was repeated 10 times. To find the accuracy achieved by each classifier, an average accuracy of all ten sets is computed. Results showed that in some cases, rice points were also detected as a weed. As a solution, Density-based spatial clustering of applications with noise (DBSCAN) was utilized with no. of neighbourhood objects equals to 8 and a radius of 50. The precision achieved by Decision Tree is 0.982, 0.953 by SVM and 0.931 by Naïve Bayes.

A CNN algorithm to classify weed and crops was presented by Dyrmann *et al.* (2016). Twenty-two different species were captured at early growth stages. Segmentation to separate green pixels and to remove unnecessary background was carried out using the excessive green method. As the algorithm proposed in this study is only translation invariant, so the training dataset was increased up to 8 times (now 50,864 images) by rotating images at intervals of 90 degrees.

Then the images were resized to 128x128 pixels. The presented algorithm consisted of 5x5 convolution layers, then batch normalization was performed using the following equation.

$$y = \frac{x-\mu}{\sqrt{\sigma^2 + \epsilon}} \gamma + \beta \quad (71)$$

Where  $\sigma$  and  $\mu$  refers to the standard deviation and mean of batch  $x$  and  $\gamma, \beta$  are trainable parameters. This step was done to make sure that input layers fall in the same range. The activation function chosen was ReLU, as it gives good results as compared to other activation functions. Besides, the architecture is also comprised of fully connected layers (for 22 species) and 2 residual layers along with max-pooling layers of size 2x2. These layers decreased the feature map size and made it translation invariant. The residual layers were determined after evaluating the filter capacity and coverage of the algorithm. Filter *Capacity* decides the complexity of features that will be mapped in the next layer and *Coverage* is an area of the image covered. These are given by:

$$Capacity = \frac{real\ filter\ size}{receptive\ field} \quad (72)$$

$$Coverage = \frac{receptive\ field}{image\ size} \quad (73)$$

where *real filter size* denotes the kernel size considering down-sampling of previous layers. Almost 1,218,614 learnable parameters were included. A 50% drop out was done just before 2 FC layers. Training images were divided into mini-batches. Each training batch consisted of 200 images. The training procedure was done after 18 epochs. The processing time for one image is about 27ms. Results showed a classification accuracy of about 86.20%. Accuracy was low for species with a smaller number of training samples.

A model named Fuzzy Real-Time Classifier (FRTC) based on visual texture features to separate weed and crop plants was discussed by Sujaritha *et al.* (2017). Inter row and intra row images were captured using two cameras one with a light ring and one without it. Then segmentation was done using green color extraction to detect inter-row weed as the weed in between two rows appears greener as compared to soil. So the red component was subtracted from the green one. If the resultant value is greater than the threshold then it means that the green component is greater than the red component thus indicating the existence of the plant. Skeletonization is used to determine the centre point (medial axes) of the leaf. Then thinning methodology is applied for pixel deletion. False branch points also occurred in some cases due to the misclassification of the binary image. A deterministic pathway is obtained for facilitating texture pattern extraction using the following equation:

$$\Delta = X \cdot \theta \quad (74)$$

where  $\Delta$  represents without branch points skeleton image,  $X$  shows skeleton image with branch points and  $\theta$  represents an image with branch points only. For broad leaves, local texture patterns, and for narrower leaves, global texture patterns were extracted by moving a circular mask of different sizes along

path  $Z$ . Four types of features including GLCM features, law's texture mask, Gabor wavelet, rotation-invariant wavelet features through radon transform were computed. The 2D Gabor wavelet function is given by:

$$H(x, y) = \exp[-\alpha^2 j \frac{(x^2 + y^2)}{2}] \cdot \exp[j \lambda \alpha^j (x \cos \theta + y \sin \theta)] \quad (75)$$

where  $\alpha = 1/\sqrt{2}$ ,  $j = 0, 1, 2, \dots$   $\theta \in [0, 2\pi]$ . The filter output at each frequency level is computed as:

$$V[j] = \sqrt{X_j^2 + \omega_j^2} \quad (76)$$

where  $X_j^2$  and  $\omega_j^2$  are the mean outputs of real and imaginary filter masks respectively. The energy and uniformity features are calculated for each sub-band. 9 out of 48 features were selected. Correct classification %age  $P_k$  for each feature  $k$  is calculated by using Euclidean classifier (Features with  $P_k$  more than 65% were selected. Through KNN 76.7% and by using Fuzzy Real-Time Classifier 91.9% weed was detected. Deep learning techniques can also be used for successful weed detection. Olsen *et al.* (2019a) studied two methods to detect weed in complex rangelands. The authors have chosen a large, public & multiclass weed dataset namely "DeepWeeds". This dataset was chosen as it contains about 17,509 images belonging to 8 different weed species. The images in this dataset are manually labelled. The techniques chosen to train a ground-based robot for weed control (known as AutoWeed for site-specific spraying in Australian rangelands) in this paper are Inception v3 and Residual neural network ResNet 50. Image data is divided into 60% - 20% - 20% for training, validation and testing. In these models, the last FC 1000 neurons are replaced with 9 (one for each target species). The mathematical representation of a convolutional layer is given in equation (77).

$$h_j^n = \max(0, \sum_{k=1}^K h_k^{n-1} * w_{kj}^n) \quad (77)$$

where  $h_j^n$  and  $h_k^{n-1}$  represents the output and input feature map respectively, and  $w_{kj}^n$  refers to the kernel. The output of both models is reduced via average pooling from  $b \times r_a \times c_a \times f_a$  (where  $r_a$  and  $c_a$  are rows and columns and  $f_a$  indicates features) to form  $b \times f_a$  and then it is further converted to  $b \times 9$ . Mathematically, average pooling is given as:

$$h_j^n(x, y) = \frac{1}{K} \sum_{\bar{x} \in N(x), \bar{y} \in N(y)} h_j^{n-1}(\bar{x}, \bar{y}) \quad (78)$$

Each processing batch contained 32 training images, each of size 224 x 224 x 3. To validate data, K fold cross-validation is done with  $k = 5$ . To evenly distribute classes in each subset, stratified random partitioning was used by the researchers. Sigmoid activation function was used to activate neurons in the output layer. Binary cross entropy was used as a loss function to calculate loss and then update parameters accordingly while training. Both models were separately trained. Results depicted that Inception v3 has an accuracy of 96.7% after 193 epochs and that for ResNet-50 is 97.6% after 155 epochs.

A research work featuring Machine Learning by DCNN for effective and successful weed detection in Bermudagrass was

proposed by Yu *et al.* (2019). For this, images of *Hedyotis corymbosa*, *Hydrocotyle* spp., and *Richardiascabra* are taken in actively growing bermudagrass. Whereas in dormant bermudagrass, images of *Poa annua* were captured along with various broadleaf weeds. At first, all images were cropped using Irfan view into 9 sub-images, each with a resolution of about 640×360 pixels. Goog LeNet and VGGNet were used for image classification, while DetectNet was used for object detection Deep Convolutional Neural Network (DCNN). Two scenarios were considered for training models. The first one is training using a dataset containing one weed species; the other one is training using multiple weed species. For the single species neural network, like the *Hydrocotyle* spp. training dataset consisted of 6000 – ve & 6000 +ve images. On the other hand, multiple species of neural networks are trained with a total of 36,000 images. While training with Detect Net for weed detection in dormant bermudagrass, all the images were resized to 1280×720 pixels. The dataset was imported in Nvidia Deep Learning GPU Training System (DIGITS). Training & testing processes implemented in DIGITS using Caffe (a framework for deep learning). The solver type chosen for this process was AdaDelta (adaptive delta) because its F1 score is better than Stochastic Gradient Descent (SGD) and Adaptive Gradient (Ada Grad). In the training of deep learning systems, you must keep on changing the hyper-parameters till the point you get your desired results. The hyper-parameters chosen in this work include a batch size of 2, Batch accumulation of 5, Exponential decay as the learning rate policy, a base learning rate of 0.1, 0.95 Gamma, 30 Training epochs. The results of validation and testing of objection detection or image classification were given in the binary confusion matrix. Precision, recall, and F1 score was calculated using given mathematical equations.

$$P = \frac{tp}{tp+fp} \quad (79)$$

$$R = \frac{tp}{tp+fn} \quad (80)$$

Where  $P$  represents precision,  $R$  indicated recall,  $tp$  shows true positives,  $fp$  represents false positives and  $fn$  shows false negatives. Precision was chosen to measure the performance, whereas recall was used to measure the effectiveness of the model. VGGNet has high precision and recall values, i.e., greater than 0.99 for the detection of *Hedyotis corymbosa*. Results suggested that GoogLeNet has low precision & is more likely to misclassify turfgrasses as weeds. The precision and recall values of DetectNet were greater than or equal to 0.9981 in the VD and TD. F1 scores of DetectNet were considerably higher than GoogLeNet and VGGNet.

## RESULTS AND DISCUSSION

Results of various supervised, unsupervised, and deep learning techniques are explained in Table 1. These tables indicate that good accuracy and successful weed detection depend not only upon the classifier but also on the features chosen for extraction and the size of the dataset. We all know that deep learning techniques provide the best results in image processing but it is not always necessary. For instance, in (Dyrmann *et al.*, 2016), a deep convolutional neural network was used for weed detection. However, the system provided an overall accuracy of 86.2%. On the other hand, many simple supervised learning techniques offered better results and accuracy above 90%. The techniques used in (Ishak *et al.*, 2008; Sujaritha *et al.*, 2017; Gao *et al.*, 2018) achieved an accuracy above 90%.

Some researchers presented novel techniques like Fast Image Processing, Automated Active Shape Matching, and Robust Crop Row Detection, which also performed better than existing image processing algorithms. The accuracy obtained by these algorithms ranges from 80% to 100%. Moreover, the accuracy achieved by using SAS PROC is also better than various algorithms. These algorithms performed better in both spectral and visual feature category, as explained by Vrindts *et al.* (2002) and Rehman *et al.* (2019). Other brief details about these research works are given in the table below.

**Table 1. A summary of various techniques used for weed detection.**

Feature category	Algorithm	The possible equation to extract feature	Accuracy/Precision	Dataset	Limitations
Spectral	3 equation made from raster data to classify blue and yellow weed. (Parra <i>et al.</i> , 2019)	$S_r = G_b/R_b$ $B_w = \left(\frac{B_b}{G_b} * R_b\right) * (G_b/R_b)$ $Y_w = \left(G_b * \frac{R_b}{B_b}\right) * (G_b/R_b)$	-	Pictures of lawn collected using drone and Arduino module	Authors did not evaluate the model at the end.
	Convolutional Neural Networks (SegNet, Unet) (Fawakherji <i>et al.</i> , 2019).	Dilation equation: $A \oplus B = \{z   (\hat{B})_z \cap A \neq \emptyset\}$ Activation function: $ReLU(x) = \begin{cases} 1 & \text{if } x > 0 \\ 0 & \text{if } x \leq 0 \end{cases}$	90%	Pictures were taken by a farming robot on a sunflower field.	Dataset is not collected with varied lighting and plant stages and hence it is not suitable for real-world applications
	K-Nearest Neighbor and Random Forest (Gao <i>et al.</i> , 2018)	$NDVI_{(\gamma_1, \gamma_2)} = \frac{NIR_{\gamma_1} - VB_{\gamma_2}}{NIR_{\gamma_1} + VB_{\gamma_2}}$	Crop precision = 94% Weeds precision =	Hyperspectral camera used for collecting maize	Precision for two of the weed species is comparatively less So

		$RVI_{(\gamma_1, \gamma_2)} = \frac{NIR_{\gamma_1}}{VB_{\gamma_2}}$	95.9%, 70.3%, 65.9%	crop and weed images.	feature selection can be improved.
	STEPDISC and DISCRIM procedure implemented in SAS (Vrindts <i>et al.</i> , 2002)	DISCRIM PROC: $p(t x) = \frac{q_t f_t(x)}{f(x)}$	Classification for sugar beet and weed >90% For Maize=15% for weed = 97% Correct detection = 92-95%	Spectrograph with digital camera used to collect images of sugar beet, maize and 7 weed species.	The algorithm did not work well under varied light conditions
<b>Spatial</b>	Detect edges by Robert's edge detector and extract weed by calculating distance with boundary points (Wu <i>et al.</i> , 2011) RCRD and Fast Image Processing (Artizzu <i>et al.</i> , 2011)	$f(i, j) = \begin{cases} 0 & 2G(i, j) < R(i, j) + B(i, j) \\ 255 & 2.5G(i, j) - R(i, j) - B(i, j) \geq 255 \\ 2.5G(i, j) - R(i, j) - B(i, j) & \text{Other} \end{cases}$ $T = \frac{\sum_{x=1}^N \sum_{y=1}^M (r \times R(x, y) + g \times G(x, y) + b \times B(x, y))}{M \times N}$ Strip-length= $\sum_{x=strip\_start}^{strip\_end} image(x, y)$	80% of crops and 95% of weed were correctly classified	Camera placed on top of tractor captured 720x576 pix maize field images.	Information about dataset is limited RCRD is time taking and hence it is not ideal for real time environment.
<b>Morpho-logical</b>	Bayes rule and KNN used for pattern recognition. Multiedit to clean boundaries (Pérez <i>et al.</i> , 2000)	Fisher Ratio: $V_{w/c} = \left  \frac{\bar{x}_w - \bar{x}_c}{\sigma_w^2 + \sigma_c^2} \right $ Bayes rule: $x \in c_i \text{ s.t. } p(c_i x) > p(c_j x) \forall j \neq i$	For crop, Bayes=89.7% KNN = 89% For weed: Bayes=74.5% KNN =79.2%	512x768 pixels images were collected from Danish cereal fields.	The algorithm does not work well under natural lighting cond. i.e. shadows and highlights.
	Area is computed by calculating no. of pixels and comparing them with set threshold. (Villa <i>et al.</i> , 2016)	$I_{bin}(x, y) = \begin{cases} 0, & I_{median}(x, y) < t \\ 1, & I_{median}(x, y) \geq t \end{cases}$ Morphological operations: $F_{mark}(x, y) = \begin{cases} 1 - I_{source}(x, y), & (x, y \text{ is on the border of } I_{source}) \\ 0, & \text{otherwise} \end{cases}$ $H_k = (H_{k-1} \otimes B) \cap G$	90% sensitivity and positive predicted values >80%	8MP camera used to collect images from Colombian vegetable farms	The authors did not provide any detailed description about area calculation. Also, the algorithm does not work well under varied illumination.
	Area computed using 8 neighbor connectivity and then comparing it with threshold. (Hlaing and Khaing, 2014)	$M(m, n) = \frac{1}{J^m K^n} \sum_{j=1}^J \sum_{k=1}^K (x_j)^m (y_k)^n F(j, k)$ Desired points: $x_j = j + 1/2$ $y_k = k + 1/2$ $I = \begin{cases} w, & area < T \\ c, & area \geq T \end{cases}$ $er = N_M / N_w * 100$	Highest weed misclassification rate = 33.3%	3648x2736 pix images collected with varying canopy size and at different times of day.	The authors didn't mention proper evaluation and validation techniques. In addition, no information about crop and weed species is given in this study.
	Automated active shape matching (AASM) (Swain <i>et al.</i> , 2011)	Mean model: $\bar{X} = \frac{1}{N} \sum_{i=0}^N X_i$ Covariance: $s = \frac{1}{N} \sum_{i=0}^N (X_i - \bar{X})(X_i - \bar{X})^T$ $SP_k = \lambda_k P_k$	Accuracy at 2-leaf stage =90%, at 3-leaf stage = 100%	1280x1024 images of black nightshade were collected using CMOS camera	This technique would not provide the desired results in case of leaf overlapping.
	Area computed by calculating no. of pixels. (Vikram <i>et al.</i> , 2018)	For RGB to Gray image: $Y = 0.299 R + 0.587 G + 0.114 B$ For image masking: $dst(I) = lowerb(I)_0 \leq src(I)_0 \leq upperb(I)_0$	-	Raspberry-Pi Camera was used to take pictures at consistent interims.	Authors did not mention any techniques for evaluation and validation of proposed algorithm. Also, the algorithm is applied on plant images taken in laboratory.
	Support Vector Machine (Murawwat <i>et al.</i> , 2018).	To extract green component of RGB image: $G = X(:, :, 2)$ Criterion for grayscale conversion: $G > T$	90%	Carrot crop dataset. (source wasn't mentioned)	The proposed model did not overcome the challenge of leaf overlapping and showed poor results in cases where the weed and crop plants are overlapped.
	K-Means Clustering. (Kaarthik and Vivek, 2018)	$W_i = \{X_{i+}, r \in W\}$ $Y_i = med\{W_i\} = med\{X_i + r : r \in W\}$	-	Pictures taken at the rate of 25 frames per second	The proposed algorithm would provide poor results in cases where crop and weed are of the same thickness, weeds have minimum edge frequencies, and there exists more than one weed plants in an image.

<b>Visual</b>	<p>SAS PROC DISCRIM,DM-H<sub>SD</sub>, DM-S<sub>SD</sub>, DM-I<sub>SD</sub>,DM- HS<sub>SD</sub>, DM-HI<sub>SD</sub>, and DM-SI<sub>SD</sub>, DM-HSI<sub>SD</sub> models based on Hue saturation and intensity (Rehman <i>et al.</i>, 2019) Support Vector Machine (Pulido <i>et al.</i>, 2017)</p>	<p>Normalization: <math display="block">p(i, j) = \frac{P(i, j, 1, 0)}{\sum_{i=0}^{q-1} \sum_{j=0}^{q-1} P(i, j, 1, 0)}</math> Decision Unit = <math display="block">\begin{cases} 1, &amp; \text{if } GR &gt; WBB \\ 0, &amp; \text{else} \end{cases}</math> <math display="block">d_{GR}^2(X^*) = (x - m_{GR})^T V_{GR}^{-1} (x - m_{GR})</math> <math display="block">S_k(X^*) = c_k + b_{k1}X_1 + b_{k2}X_2 + \dots + b_{kp}X_p</math> GLCM: <math display="block">C_{\Delta x, \Delta y}(i, j) = \sum_{p=1}^n \sum_{q=1}^m \begin{cases} 1, &amp; \text{If } I(p, q) = i \text{ and } I(p + \Delta x, q + \Delta y) \\ 0, &amp; \text{otherwise} \end{cases}</math> Min: <math>w^2 = \phi(w, b)</math> Subject to: <math>y_i[w, x + b] - 1 \geq 0</math></p>	<p>DM- HSI<sub>SD</sub> achieved 94.98% on training and 93.80% on testing dataset.</p>	<p>1280×1024 images are collected at real time from 2 cameras to detect golden rod in wild blueberry. 250 images of spinach and chard crops using 8MP camera.</p>	-
<b>Multiple features</b>	<p>KNN, Fuzzy real-time classification technique (Sujaritha <i>et al.</i>, 2017).</p>	<p>Skeletonization: <math>\Delta = X \cdot \theta</math> Gabor Wavelet: <math>H(x, y) = \exp[-\alpha^2 j \frac{(x^2 + y^2)}{2}] \cdot \exp[j \lambda \alpha^j (x \cos \theta + y \sin \theta)]</math> Filter output: <math>V[j] = \sqrt{X_j^2 + \omega_j^2}</math></p>	92.9%	<p>A web camera captured 3264x2448 inter-row images. A digital RGB camera capture intra-row images in sugarcane fields.</p>	-
Support Vector Machine (Ishak <i>et al.</i> , 2008)	<p>RBF kernel: <math>K(x, y) = \exp\left(-\frac{\ x-y\ ^2}{2\sigma^2}\right)</math> Optimization: <math display="block">W(\alpha) = \sum_{i=1}^M \alpha_i - \frac{1}{2} \sum_{i=1}^M \sum_{j=1}^M \alpha_i \alpha_j y_i y_j K(x_i, x_j)</math></p>	100%	<p>200 images, 100 narrow and 100 broad leaf</p>	<p>The dataset used in the process is extremely small and so the model may not provide good results for large dataset.</p>	
Probabilistic models and K-means clustering (Kodagoda <i>et al.</i> , 2008)	<p>K-means formula: <math display="block">J = \sum_{j=1}^k \sum_{i=1}^n \ x_i^{(j)} - c_j\ ^2</math> Mahalanobis distance: <math display="block">D = \sqrt{(x - m)^T \cdot C^{-1} \cdot (x - m)}</math></p>	<p>For wheat: 85% detection rate, 82% false alarm rate For lolium: 26% detection rate.</p>	<p>Images were taken in laboratory with a camera setup and three potted plant species wheat, biden and lolium.</p>	<p>The proposed model based on k-means is applied on laboratory images and so it is not trained for real time environment.</p>	
Inception-v3, ResNet- 50 (Olsen <i>et al.</i> , 2019a)	<p>Convolutional layer: <math display="block">h_j^n = \max\left(0, \sum_{k=1}^K h_k^{n-1} * w_{kj}^n\right)</math> Average pooling: <math display="block">h_j^n(x, y) = \frac{1}{K} \sum_{\bar{x} \in N(x), \bar{y} \in N(y)} h_j^{n-1}(\bar{x}, \bar{y})</math></p>	<p>Inception-v3: 95.1%. ResNet-50: 95.7%</p>	<p>DeepWeeds dataset which comprises of 17,509 multiclass images. (Olsen, 2020)</p>	<p>The author did not train the model on field images and so the model may not provide efficient classification results in real- time environment.</p>	
Harris corner detection, Decision Tree, SVM and Naïve Bayes and DBSCAN (to filter false- positives) (Cheng and Matson, 2015)	<p>Harris detector: <math display="block">E(u, v) = (u, v) M(u, v)^T</math> <math display="block">M = \sum_{x, y} w(x, y) \begin{bmatrix} I_x^2 &amp; I_x I_y \\ I_x I_y &amp; I_y^2 \end{bmatrix}</math></p>	<p>Precision by Decision Tree is 0.982, 0.953 by SVM and 0.931 by Naïve Bayes.</p>	-	<p>In future the proposed technique can be improved to detect various other weed types in rice crop or any other crop. Also, the model can be implemented on a robotic system.</p>	
Hough transform, KNN (Åstrand and Baerveldt, 2002)	<p>Opening: <math>f \circ s = (f \ominus s) \oplus s</math> Line: <math>y_i = ax_i + b</math> Perspective Transformation: <math>A\alpha + Bs + C</math></p>	<p>97% classification rate by using all features and 5NN classifier.</p>	<p>3 sets of images collected using 2 cameras. One for row recognition other for single-crop detection in sugar beet fields.</p>	-	
Support Vector Machine (Ahmed <i>et al.</i> , 2012)	<p>Form factor = <math>4\pi \frac{\text{area}}{\text{perimeter}^2}</math> Elongatedness = <math>\frac{\text{area}}{\text{thickness}^2}</math> Convexity = <math>\frac{\text{convex\_perimeter}}{\text{perimeter}}</math> Solidity = <math>\frac{\text{convex\_area}}{\text{area}}</math> <math display="block">K(x_i, x_j) = \exp\left(-\gamma \ x_i - x_j\ ^2\right), \gamma &gt; 0</math></p>	>97%	<p>1200x768 pix images consisting of chilli crop and 5 weed species, obtained from chilli fields of Bangladesh</p>	-	

GoogLeNet, VGGNet and DetectNet(Yu <i>et al.</i> , 2019)	$P = \frac{tp}{tp + fp}$ $R = \frac{tp}{tp + fn}$	VGGNet> 95% DetectNet>99 %	36,000 images of res. 1920×1080 of brmudagrass along with various weed species were collected from April to September and then in February, at different time of day.	The algorithms require large image dataset to train properly and so it may not generate good results on a dataset containing a few thousand images.
Deep Convolutional Neural Network. (Dyrmann <i>et al.</i> , 2016)	batch normalization: $y = \frac{x-\mu}{\sqrt{\sigma^2 + \epsilon}} \gamma + \beta$ $Capacity = \frac{real\ filter\ size}{receptive\ field}$ $Coverage = \frac{receptive\ field}{image\ size}$	86.2%	10413 images of 22 different plant species at early growth stages were obtained from datasets of 6 different sources.	Deep learning techniques require extremely large datasets to achieve an accuracy of above 90%.
Area and moment of order computation. (Masuda <i>et al.</i> , 2010)	$G > 150 \wedge G - R < 30 \wedge G - B > 80$ Area: $A = 255 \times \frac{N_{near}}{W_{width} \times W_{height}}$ Moment of order: $M_{m,n} = 225 \times \frac{\sum_{x,y}(x-cgx)^m(y-cgy)^n I(x,y)}{\max[\sum_{x,y}(x-cgx)^m(y-cgy)^n I(x,y)]}$	-	640*480 pix images of paddy rice fields were collected and then transformed to BMP format.	No accuracy, correct detection rate or false detection rate were given and hence it is difficult to evaluate the study.

**Conclusion:** The main purpose of weed detection is to improve both environmental and economic conditions. Excess herbicide application on the entire field causes damage by developing resistance in weed plants and injecting harmful chemicals into the soil. Through automatic weed detection, we can not only reduce labor costs but also the machine will detect weed and then spray herbicide solely on the weed plants. This is beneficial to the soil and environment and the country’s economic conditions.

The various ways discussed above can be implemented to detect weed automatically both in field and laboratory conditions. Nevertheless, the implementation highly depends upon the plant features and the desired results. If there is a suitable difference between the color features of both weed and crop, one can rely on the algorithm based on color features for classification. In case if the difference is not suitable, then one should combine the color features along with some other distinguished features. For example, if the crop plants have narrow leaves and the weed plants have broad leaves, then it is better to choose area features for successful identification.

If one wants to detect both inter-row and intra-row weed, it is more convenient to use color features for weed within two crop rows because, in that case, one only needs to find the green weed plant against the soil (background). For inter-row weed, the best way is to detect rows first by capturing images using a camera mounted at some height. Once rows are detected, one can separate crop and weeds based on features that provide maximum information about them.

Another important factor in the study of weed detection models is the size of the dataset used to train and test the model. Models based on deep learning techniques like ANN (Artificial Neural Network), CNN, and DCNN (Deep Convolutional Neural Network) require extremely large datasets to get properly trained. For instance, if the dataset

consists of images less than 10000, then the model might not be able to give the desired results. On the other hand, algorithms like KNN give the best results with small datasets. Similarly, the Random Forest algorithm provides good results if the dataset contains multiple classes as compared to SVM, which is known to give better results with binary classification problems.

Based on these distinguishing features, a classification algorithm is applied to identify crops and weeds from the images. In the above-presented research works, algorithms are also tested at the end. This was done either by performing K-fold cross-validation or by calculating precision, recall, specificity, and sensitivity. All these methods are used for evaluation.

**REFERENCES**

Ahmed, F., H.A. Al-Mamun, A.S.M.H. Bari, E. Hossain and P. Kwan. 2012. Classification of crops and weeds from digital images: a support vector machine approach. *Crop Prot* 40:98-104.

Artizzu, X.P.B., A. Ribeiro, M. Guijarro and G. Pajares. 2011. Real-time image processing for crop/weed discrimination in maize fields. *Comput. Electron. Agric.* 75:337-346.

Åstrand, B. and A.-J. Baerveldt. 2002. An agricultural mobile robot with vision-based perception for mechanical weed control. *Auton. Robots* 13:21-35.

Bakhshipour, A., A. Jafari, S.M. Nassiri and D. Zare. 2017. Weed segmentation using texture features extracted from wavelet sub-images. *Biosyst. Eng.* 157:1-12.

Cheng, B. and E.T. Matson. 2015. A feature-based machine learning agent for automatic rice and weed discrimination. In: L. Rutkowski, M. Korytkowski, R. Scherer, R. Tadeusiewicz, L.A. Zadeh, and J.M. Zurada

- (eds.), *Artificial Intelligence and Soft Computing*. Springer International Publishing, Cham. pp. 517-527.
- Desai, H.M. and V. Gandhi. 2014. A survey: background subtraction techniques. *Int. J. Sci. Eng. Res.* 5:1365-1367.
- Dyrmann, M., H. Karstoft and H.S. Midtby. 2016. Plant species classification using deep convolutional neural network. *Biosyst. Eng.* 151:72-80.
- Emery, A. 2012. Exponential Population Growth | Kivu. Exponential population growth. Available at <https://kivu.com/exponential-population-growth/>.
- Fawakherji, M., A. Youssef, D. Bloisi, A. Pretto and D. Nardi. 2019. Crop and weeds classification for precision agriculture using context-independent pixel-wise segmentation. *2019 Third IEEE International Conference on Robotic Computing (IRC)*. IEEE, Naples, Italy, Italy. pp.146-152.
- Food and population: FAO looks ahead. 2000. Food and Agriculture Organization of United Nations. Available at <http://www.fao.org/NEWS/2000/000704-e.htm>.
- Gao, J., D. Nuyttens, P. Lootens, Y. He and J.G. Pieters. 2018. Recognising weeds in a maize crop using a random forest machine-learning algorithm and near-infrared snapshot mosaic hyperspectral imagery. *Biosyst. Eng.* 170:39-50.
- Gerhards, R. and S. Christensen. 2003. Real-time weed detection, decision making and patch spraying in maize, sugarbeet, winter wheat and winter barley. *Weed Res.* 43:385-392.
- Hameed, S. and I. Amin. 2018. Detection of Weed and Wheat Using Image Processing. *2018 IEEE 5th International Conference on Engineering Technologies and Applied Sciences (ICETAS)*. IEEE, Bangkok, Thailand. pp.1-5.
- Hamuda, E., B. Mc Ginley, M. Glavin and E. Jones. 2017. Automatic crop detection under field conditions using the HSV color space and morphological operations. *Comput. Electron. Agric.* 133:97-107.
- Hlaing, S.H. and A.S. Khaing. 2014. Weed and crop segmentation and classification using area thresholding. *Int. J. Res. Eng. Technol.* 3:375-382.
- Ishak, A.J., M.M. Mustafa, N.M. Tahir and A. Hussain. 2008. Weed detection system using support vector machine. *2008 International Symposium on Information Theory and Its Applications*. IEEE, Auckland, New Zealand. pp.1-4.
- Jones, B. 2017. The Earth's population is going to reach 9.8 billion by 2050. World Economic Forum. Available at <https://www.weforum.org/agenda/2017/08/the-earths-population-is-going-to-reach-9-8-billion-by-2050/>.
- Kaarthik, K. and C. Vivek. 2018. Weed remover in agricultural field through Image processing. *Int. J. Pure Appl. Math.* 118:393-398.
- Kazmi, W., F. Garcia-Ruiz, J. Nielsen, J. Rasmussen and H.J. Andersen. 2015. Exploiting affine invariant regions and leaf edge shapes for weed detection. *Comput. Electron. Agric.* 118:290-299.
- Kodagoda, S., Z. Zhang, D. Ruiz and G. Dissanayake. 2008. Weed detection and classification for autonomous farming. *I\*PROMS*, Steyr-Gleink, Austria. pp.1-6.
- Lee, W.S., V. Alchanatis, C. Yang, M. Hirafuji, D. Moshou and C. Li. 2010. Sensing technologies for precision specialty crop production. *Comput. Electron. Agric.* 74:2-33.
- Liu, B. and R. Bruch. 2020. Weed detection for selective spraying: a review. *Curr. Robot. Rep.* 1:19-26.
- Masuda, R., K. Nomura and K. Nakayama. 2010. Rice plant detection in pre-heading term for autonomous robot navigation. *XVIIth World Congress of the International Commission of Agricultural and Biosystems Engineering (CIGR)*. pp.1-8.
- Murawwat, S., A.-J. Qureshi, S. Ahmad and Y. Shahid. 2018. Weed detection using SVMs. *Eng. Technol. Appl. Sci. Res.* 8:2412-2416.
- Nandhini, P.S. and S. Ravishankar. 2019. A study on weed detection techniques. *Int. J. Inf. Syst. Comput. Sci.* 8:25-29.
- Neto, J.C., G.E. Meyer, D.D. Jones and A.K. Samal. 2006. Plant species identification using elliptic fourier leaf shape analysis. *Comput. Electron. Agric.* 50:121-134.
- Olsen, A. 2020. *AlexOlsen/DeepWeeds*.
- Olsen, A., D.A. Konovalov, B. Philippa, P. Ridd, J.C. Wood, J. Johns, W. Banks, B. Girgenti, O. Kenny, J. Whinney, B. Calvert, M.R. Azghadi and R.D. White. 2019. Deep Weeds: a multiclass weed species image dataset for deep learning. *Sci. Rep.* 9:1-14
- Parra, L., V. Torices, J. Marín, P.V. Mauri and J. Lloret. 2019. The use of image processing techniques for detection of weed in lawns. *ICONS 2019: The Fourteenth International Conference on Systems*. The International Academy, Research and Industry Association, Valencia, Spain. pp.50-55.
- Pérez, A.J., F. López, J.V. Benlloch and S. Christensen. 2000. Colour and shape analysis techniques for weed detection in cereal fields. *Comput. Electron. Agric.* 25:197-212.
- Peters, J., B.D. Baets, N.E.C. Verhoest, R. Samson, S. Degroove, P.D. Becker and W. Huybrechts. 2007. Random forests as a tool for ecohydrological distribution modelling. *Ecol. Model.* 207:304-318.
- Pulido, C., L. Solaque and N. Velasco. 2017. Weed recognition by SVM texture feature classification in outdoor vegetable crop images. *Ing. E Investig.* 37:68-74.
- Rasti, P., A. Ahmad, S. Samiei, E. Belin and D. Rousseau. 2019. Supervised image classification by scattering transform with application to weed detection in culture crops of high density. *Remote Sens.* 11:1-16.
- Rehman, T.U., Q.U. Zaman, Y.K. Chang, A.W. Schumann and K.W. Corscadden. 2019. Development and field evaluation of a machine vision based in-season weed

- detection system for wild blueberry. *Comput. Electron. Agric.* 162:1–13.
- Saber, M., W.S. Lee, T.F. Burks, J.K. Schueller, C.A. Chase, G.E. MacDonald and G.A. Salvador. 2015. Performance and evaluation of intra-row weeder ultrasonic plant detection system and pinch-roller weeding mechanism for vegetable crops. *2015 ASABE International Meeting. American Society of Agricultural and Biological Engineers.* pp.1-9.
- Singh, A., B. Ganapathysubramanian, A.K. Singh and S. Sarkar. 2016. Machine learning for high-throughput stress phenotyping in plants. *Trends Plant Sci.*21:110-124.
- Slaughter, D.C., D.K. Giles and D. Downey. 2008. Autonomous robotic weed control systems: a review. *Comput. Electron. Agric.* 61:63-78.
- Sujaritha, M., S. Annadurai, J. Satheeshkumar, S. Kowshik Sharan and L. Mahesh. 2017. Weed detecting robot in sugarcane fields using fuzzy real time classifier. *Comput. Electron. Agric.* 134:160-171.
- Swain, K.C., M. Nørremark, R.N. Jørgensen, H.S. Midtby and O. Green. 2011. Weed identification using an automated active shape matching (AASM) technique. *Biosyst. Eng.* 110:450-457.
- Tejeda, A.J.I. and R.C. Castro. 2019. Algorithm of weed detection in crops by computational vision. *2019 International Conference on Electronics, Communications and Computers (CONIELECOMP).* IEEE, Cholula, Mexico. pp.124–128.
- Tiwari, O., V. Goyal, P. Kumar and S. Vij. 2019. An experimental set up for utilizing convolutional neural network in automated weed detection. *2019 4th International Conference on Internet of Things: Smart Innovation and Usages (IoT-SIU).* IEEE, Ghaziabad, India. pp.1-6.
- Tyystjärvi, E., M. Nørremark, H. Mattila, M. Keränen, M. Hakala-Yatkin, C.-O. Ottosen and E. Rosenqvist. 2011. Automatic identification of crop and weed species with chlorophyll fluorescence induction curves. *Precis. Agric.* 12:546-563.
- Ullah, A., N. Mohd Nawi, A. Arifianto, I. Ahmed, M. Aamir and S.N. Khan. 2019. Real-time wheat classification system for selective herbicides using broad wheat estimation in deep neural network. *Int. J. Adv. Sci. Eng. Inf. Technol.* 9:153–158.
- Vikhram, G.Y.R., R. Agarwal, R. Uprety and V.N.S. Prasanth. 2018. Automatic weed detection and smart herbicide sprayer robot. *Int. J. Eng. Technol.*7:115-118.
- Villa, M.A.M., L.E.S. Guzmán and C.A.P. Rojas. 2016. Machine vision system for weed detection using image filtering in vegetables crops. *Rev. Fac. Ing. Univ. Antioquia.* 124–130.
- Vrindts, E., J. De Baerdemaeker and H. Ramon. 2002. Weed detection using canopy reflection. *Precis. Agric.* 3:63-80.
- Wang, A., W. Zhang and X. Wei. 2019. A review on weed detection using ground-based machine vision and image processing techniques. *Comput. Electron. Agric.* 158:226-240.
- Wang, L. 2010. Identification based on color and texture of the soybean leaf nitrogen diagnostic model. *Proceedings of the 29th Chinese Control Conference.* IEEE, Beijing, China. pp.2849-2852.
- Wu, X., W. Xu, Y. Song and M. Cai. 2011. A detection method of weed in wheat field on machine vision. *Procedia Eng.* 15:1998-2003.
- Young, D.L., T.J. Kwon, E.G. Smith and F.L. Young. 2003. Site-specific herbicide decision model to maximize profit in winter wheat. *Precis. Agric.* 4:227-238.
- Yu, J., S.M. Sharpe, A.W. Schumann and N.S. Boyd. 2019. Deep learning for image-based weed detection in turfgrass. *Eur. J. Agron.* 104:78-84.

**APPENDIX: Nomenclature**

---

RF	Random forest
KDE	Kernel Density Estimation
VGG	Visual Geometry Group
NDVI	Normalized Difference Vegetation Index
ExG	Excess Green
CIVE	Color Index of Vegetation Extraction
mIOU	mean Intersection-Over-Union
RVI	Ratio Vegetation Index
PCA	Principal Component Analysis
SAS	Statistical Analysis System
RCRD	Robust crop row detection
GLCM	Grey level co-occurrence matrix
FRTC	Fuzzy Real Time Classifier
DM-HSD	(STEPDISC) Data Model for Hue
FFT	Fast Fourier Transform
DCNN	Deep Convolutional Neural Network
GMM	Gaussian Mixture Model
CNN	Convolutional Neural Networks
FC	Fully connected
ExG	Excess Red
NDI	Normalized Difference Index
ReLU	Rectified Linear Unit
ROI	Region of interest
OOB	out-of-bag
KNN	K-nearest Neighbor
NIR	Near Infra-Red
FIP	Fast Image Processing
HSI	Hue-Saturation-Intensity
MD	Mahalanobis Distance
SVM	Support Vector Machine
RBF	Radial Basis Function

---